Available online www.jsaer.com

***Journal of Scientific and Engineering Research*, 2018, 5(10):277-289**

Research Article

ISSN: 2394-2630
CODEN(USA): JSERBR

Effects of Slip Conditions on MHD Diffusive Reactive Flow with Radiative Heat Transfer Past a Vertical Porous Plate

Amos Emeka*, Numesubo Gift Alexander

Department of Mathematics, Rivers State University, Port Harcourt, Nigeria

Abstract In this paper, we examine the slip effects on the MHD boundary layer flow and radiative heat transfer past a vertical porous plate embedded in chemically reactive fluid. The balanced nonlinear coupled system of partial differential equations governing the flow of momentum, energy and concentration is transformed into a system of ordinary differential equation in dimensionless form. The resulting dimensionless equations are solved analytically by the regular perturbation method to obtain approximate solutions for the velocity, temperature and concentration fields. Numerical results are also obtained to validate the analytical results obtained by using fifth-order Runge-Kutta Fehlberg numerical experiments implemented in Maple 18. The remarkable effects of magnetic, thermal radiation, suction and injection, and Grashof number on the flow variables as well as on skin friction, heat and mass transfer rates are discussed in graphical and tabular forms.

Keywords Slip condition, Radiative heat, Magnetohydrodynamics, Porous plate, chemical reaction

1. Introduction

In the past and over the years, the efficacy and applicability of the MHD boundary layer flow has had far reaching effects in science and engineering and even in medicine. In engineering, MHD is used to tackle vital engineering problems such as plasma confinement, liquid-metal cooling of nuclear reactors, electromagnetic casting, MHD pumps and generators. In medicine, MHD is mainly applied in magnetic drug targeting in cancer research. The study of MHD boundary layer flow of an incompressible viscous fluid together with heat and mass transfer processes over a vertical porous plate has been an active and juicy field of study of hydrodynamics to many researchers due to the abundance of practical applications in chemical and manufacturing processes.

Since the pioneering work of Blasius [1] on the boundary layers in fluids with little friction, many researchers have explored the boundary layers MHD slip flows of viscous fluids over vertical porous plates. Wadsworth [2] investigated the slip effects in a confined rarefied gas and solved the resulting interaction models with a finite difference Navier-Strokes method using slip boundary conditions. Aral and Kaylon [3] observed the slip effects of temperature and surface roughness on time dependent development of wall slip in steady tensional flow of concentrated suspensions and the behaviour of the solution of the problem by the steady state analysis. Sahraoui and Kaviany [4] investigated the slip and no-slip temperature boundary conditions at the interface of porous, plain media, Abbey and Bestman [5] investigated the slip flow of two-component plasma model with radiative heat transfer and solved the modeled equations by deriving various asymptotic solutions since exact solutions are inconceivable. Rao and Rajagopal [6] investigated the effect of slip boundary condition on the flow of fluids in a channel; Mebine [7] investigated the thermosolutal MHD flow with radiative heat transfer past an oscillating plate in a chemically active fluid and solved the modeled equations by Laplace transform technique on the assumption of an optically thin medium, and linear differential approximation model for the radiative flux. Matin and Boyd [8] investigated the effects of slip on momentum and heat transfer in a laminar boundary layer flow over a flate plate. Hayet et al. [9] discussed the peristaltic flow of a third order fluid in an asymmetric channel in the presence of slip condition without heat and mass transfer effects. Yazdi et al. [10] studied the slip

flow boundary conditions. Mebine [11] investigated the double diffusive convective MHD flow past a vertical porous plate in a chemically active fluid with radiative heat transfer in the presence of viscous work and heat source and solved the resulting nonlinear dimensionless equations by asymptotic analysis technique giving approximate analytical solutions for the unsteady velocity, temperature and concentration. Abas at al. [12] examined the heat transfer problem around an oscillatory infinite sheet with slip boundary condition, Fang et al. [13] examined the slip MHD boundary layer over a stretching sheet, Ahuja and Singh [14] investigated slip velocity of concentrated suspensions in coquette flow and provided a simple methodology for the determination of slip velocity. Cao and Baker [15] investigated the mixed convective flow of heat transfer from a vertical plate by considering velocity and temperature jumps boundary conditions. Hayat et al. [16] studied the velocity slip, temperature and concentration jumps conditions and found that the effect of fluid wall interaction is also important. Pal and Talukdar [17] presented an analytical solution of unsteady MHD convection heat and mass transfers past a vertical permeable plate with thermal radiation and chemical reaction in the presence of slip at the boundary by sing perturbation analysis. Bhattacharyya et al. [18] investigated the MHD boundary layer slip flow and heat transfer over a flat plate and solved the governing equations by the shooting method. Yazdi et al. [19] studied thew effect of permeability parameter on the slip flow regime and showed that mass suction has a significant effect on the fluid velocity adjacent to the wall in the presence of partial slip. Mebine [20] investigated the MHD velocity slip boundary layer flow over a plane plaque and solved the resulting nonlinear system of differential equations by the Leibnitz-Maclaurin's method (LMM) via successive differential coefficients (SDC).

The aim of the present paper is to investigate the combined effects of magnetic field and suction/blowing. Moreover, the effects of hydrodynamic slip, thermal slip and mass slip on one-dimensional steady MHD diffusive reactive flow with radiative heat transfer past a vertical plate that is porous are analyzed using dimensionless variables, the momentum, concentration and energy equations are written in dimensionless forms. These equations are solved analytically by the regular perturbation method and numerically by the fifth order Runge-Kutta-Fehlberg numerical method implemented in Maple 18. The effects of the physical parameters on the flow variables are investigated and discussed with the help of their graphical and tabular representations. Also, the effects of these parameters on the skin friction, heat and mass transfer rates are presented in tabular forms.

2. Formulation of the Problem

We consider a diffusive reactive flow of a one-dimensional steady laminar boundary layer flow of a fluid of density ρ that is incompressible and chemically active over a vertical plate that is porous with radiative heat transportation in the presence of magnetic field and heat transfer. The equations governing the boundary layer MHD flow for the momentum, concentration and energy transfers are written thus:

$$v\frac{du}{dy}=\nu\frac{d^2u}{dy^2}-\frac{\sigma_c B_0^2}{\rho}(u-u_\infty)+g\beta_+(T-T_\infty)+g\beta_-(C-C_\infty) \tag{1}$$

$$v\frac{dT}{dy}=\alpha_d\frac{d^2T}{dy^2}-\frac{1}{\rho c_p}\frac{dq}{dy} \tag{2}$$

$$v\frac{dC}{dy}=D\frac{d^2C}{dy^2}-k_r(C-C_\infty) \tag{3}$$

and where the radiative heat flux for an optically thin medium is given by

$$\frac{dq}{dy}=4\sigma\alpha\left(T^4-T_\infty^4\right)\approx 16\sigma\alpha T_\infty^3(T-T_\infty) \tag{4}$$

Here u and v are the component velocities along the $x-$ and $y-$axes, respectively; σ_c, the electrical conductivity; B_0, applied magnetic field; ρ, fluid density; μ, dynamic viscosity; ν, kinematic viscosity; β_+, thermal volume expansion; β_-, mass volume expansion; α_d, thermal diffusivity; c_p, heat capacity at constant

pressure; D, mass diffusivity; k_r, first-order chemical reaction; T, fluid temperature; C, mass concentration; α, penetration depth; σ, Boltzmann constant, and g, acceleration due to gravity.

The appropriate boundary conditions to the equations (2) – (4) are given as follows;

$$\text{for } y=0: u=L_u\frac{du}{dy}, v=v_w, T=T_w+D_T\frac{dT}{dy}, C=C_w+D_C\frac{dC}{dy}$$
$$\text{as } y\to\infty:\ u\to u_\infty, T\to T_\infty, C\to C_\infty \tag{5}$$

where

$L_u, D_T, D_C, v_w, T_w, C_w$ accounts for hydrodynamic slip factor, mass slip factor, wall velocity, wall temperature, and wall concentration respectively, $u_\infty, T_\infty, C_\infty$ are respectively the ambient velocity, ambient temperature, and ambient concentration.

To further facilitate the analyses, the following dimensionless variables and physical parameters are employed:

$$Y=\frac{yu_\infty}{\nu}, U=\frac{u}{u_\infty}, \theta=\frac{T-T_\infty}{T_w-T_\infty}, C=\frac{C-C_\infty}{C_w-C_\infty}, S=\frac{v_w}{u_\infty},$$
$$M=\frac{\sigma_c\nu B_0^2}{\rho u_\infty^2}, Gr=\frac{\nu g\beta_T(T_w-T_\infty)}{u_\infty^3}, Gc=\frac{\nu g\beta_c(C_w-C_\infty)}{u_\infty^3},$$
$$\Pr=\frac{\nu}{\alpha_d}, Sc=\frac{\nu}{D}, N=\frac{16\alpha\nu T_\infty^3}{\rho c_p}, R=\frac{k_r\nu}{u_\infty^2}$$
$$L=\frac{L_u u_\infty}{\nu}, D_T^t=\frac{D_T u_\infty}{\nu}, D_C^c=\frac{D_C u_\infty}{\nu}. \tag{6}$$

Therefore, using (6) in equations (1) to (3), the dimensionless governing equations are:

$$\frac{d^2U}{dY^2}+S\frac{dU}{dY}-M\,(U-1)+Gr\theta+GcC=0 \tag{7}$$

$$\frac{1}{\Pr}\frac{d^2\theta}{dY^2}+S\frac{d\theta}{dY}-N\theta=0 \tag{8}$$

$$\frac{1}{Sc}\frac{d^2C}{dY^2}+S\frac{dC}{dY}-RC=0 \tag{9}$$

With the appropriate boundary conditions as

$$U=L\frac{dU}{dY}, \theta=1+D_T^t\frac{d\theta}{dY}, C=1+D_C^c\frac{dC}{dY} \quad \text{at} \quad Y=0,$$
$$U\to 1, \theta\to 0, C\to 0 \quad as \quad Y\to\infty \tag{10}$$

The parameters entering the problem are $S, M, Gr, Gc, \Pr, Sc, N, R, L, D_T^t, D_C^c$, which represents suction parameter when $S>0$ or injection when $S<0$, magnetic parameter, thermal Grashof number, mass Grashof number, Prandtl number, Schmidt number, thermal radiation, reaction parameter, hydrodynamic slip factor parameter, thermal slip factor parameter, and mass slip factor parameter, respectively.

The mathematical formulation embodies equations (7) - (9) together with the boundary conditions (10). The mathematical formulations are now complete.

3. Methods of Solution

Two methods are considered, viz: regular perturbation and finite difference numerical methods via Runge-Kutta Fehlberg method.

3.1 Regular Perturbation Method

The equations (7) – (9) are coupled nonlinear differential equations. In seeking approximate analytical solutions to validate numerical solutions of such nonlinear couple equations, it is a usual practice to expand the field variables in series about a small parameter. This method is usually called regular perturbation. Fortunately, the Eckert number, which is measure of the rigor of heat convection, is always small (i.e. $Ec\ll 1$) in most incompressible fluids. Therefore, the approximate solutions are adopted as follows:

$$\Phi(Y)=\Phi_0(Y)+Ec\Phi_1(Y)+0(E_C^2), \tag{11}$$

Where Φ stands for any of U, θ or C.

Using equation (11) in equations (7) – (9) together with the associated boundary conditions (10), gives the perturbed equations. Therefore, the equations for E_C^0 are given by the following:

$$\frac{d^2U_0}{dY^2} + S\frac{dU_0}{dY} - M\left(U_0 - 1\right) + Gr\theta_0 + GcC_0 = 0, \tag{12}$$

$$\frac{1}{\Pr}\frac{d^2\theta_0}{dY^2} + S\frac{d\theta_0}{dY} - N\theta_0 = 0, \tag{13}$$

$$\frac{1}{Sc}\frac{d^2C_0}{dY^2} + S\frac{dC_0}{dY} - RC_0 = 0, \tag{14}$$

$$U_0 = L\frac{dU_0}{dY}, \theta_0 = 1 + D_T^t\frac{d\theta_0}{dY}, C_0 = 1 + D_C^c\frac{dC_0}{dY} \quad \text{at} \quad Y = 0,$$
$$U_0 \to 1, \theta_0 \to 0, C_0 \to 0 \quad as \quad Y \to \infty \tag{15}$$

For E_C, the governing equations are the following:

$$\frac{d^2U_1}{dY^2} + S\frac{dU_1}{dY} - MU_1 + Gr\theta_1 + GcC_1 = 0, \tag{16}$$

$$\frac{1}{\Pr}\frac{d^2\theta_1}{dY^2} + S\frac{d\theta_1}{dY} - N\theta_1 = 0, \tag{17}$$

$$\frac{1}{Sc}\frac{d^2C_1}{dY^2} + S\frac{dC_1}{dY} - RC_1 = 0, \tag{18}$$

$$U_1 = L\frac{dU_1}{dY}, \theta_1 = D_T^t\frac{d\theta_1}{dY}, C_1 = D_C^c\frac{dC_1}{dY} \quad \text{at} \quad Y = 0, \tag{19}$$
$$U_1 \to 0, \theta_1 \to 0, C_1 \to 0 \quad as \quad Y \to \infty$$

With boundedness and some bit of straight algebra, the solutions to the equations (12) - (18) are given as follows:

$$\theta(Y) = \frac{1}{1 + D_T^t m_1}\exp\left(-m_1 Y\right), \tag{20}$$

$$C(Y) = \frac{1}{1 + D_C^c r_1}\exp\left(-r_1 Y\right), \tag{21}$$

$$U(Y) = 1 + \alpha_1\exp\left(-n_1 Y\right) - \alpha_2\exp\left(-m_1 Y\right) - \alpha_3\exp\left(-r_1 Y\right), \tag{22}$$

where

$$m_1 = \frac{\Pr S}{2} + \sqrt{\frac{\Pr^2 S^2}{4} + \Pr\left(N\right)},$$

$$r_1 = \frac{Sc}{2} + \sqrt{\frac{Sc^2 S^2}{4} + ScR}.$$

$$n_1 = \frac{S}{2} + \sqrt{\frac{S^2}{4} + M}$$

$$\alpha_1 = -\frac{1}{1 + Ln_1} + \frac{Gr\left(1 + m_1\right)}{\left(1 + Ln_1\right)\left(1 + m_1 D_T^t\right)\left(m_1^2 - Sm_1 - M\right)} + \frac{Gc\left(1 + r_1\right)}{\left(1 + Ln_1\right)\left(1 + r_1 D_C^c\right)\left(r_1^2 - Sr_1 - M\right)},$$

$$\alpha_2 = \frac{Gr}{\left(1 + m_1 D_T^t\right)\left(m_1^2 - Sm_1 - M\right)},$$

$$\alpha_3 = \frac{Gc}{\left(1 + r_1 D_C^c\right)\left(r_1^2 - Sr_1 - M\right)}$$

3.2. Shear Stress, Heat and Mass Transfer Fluxes

When the plate moves through a fluid, it is necessary to know the shear stress or skin friction on the wall of the plate. This is given as follows:

$$\tau_s = \frac{\tau}{\rho u_\infty^2} = \left.\frac{dU}{dY}\right|_{Y=0}. \tag{23}$$

Due to the long and complex nature of the expression, it is not stated here to save space.

The rate of heat transfer, q_T, between the fluid and the wall of the plate is given by:

$$q_\theta = \frac{\nu q_T}{k_T u_\infty (T_w - T_\infty)} = -\left.\frac{d\theta}{dY}\right|_{Y=0}. \tag{24}$$

The rate at which mass is transferred across the plate in the non-dimensional form is given by;

$$q_C = \frac{\nu q_c}{D u_\infty (C_w - C_\infty)} = -\left.\frac{dC}{dY}\right|_{Y=0}. \tag{25}$$

3.3. Runge-Kutta-Fehlberg Numerical Method

The numerical method used in this research is the *Runge-Kutta Fehlberg* method, which produces a solution whose accuracy is to the fifth order. The implementation of the numerical scheme is done in Maple 18, where the default numerical method is the *Runge-Kutta Fehlberg* method in the dissolve command.

In solving Boundary Value or Initial Value Problems numerically, one way to guarantee accuracy in the solution is to solve the problem twice using different step sizes h and $h/2$ and compare the answers at the mesh points that correspond to the larger step size. But this procedure is much more cumbersome and stressful as it requires a lot of computation for the smaller step size and must be repeated if it determined that the agreement is not good enough.

To get across the problem so as to try to resolve this problem, the Fifth-order *Runge-Kutta-Fehlberg* method (denoted RKF45) is used, whose procedure determines whether or not, the proper step size h is being used. It simply finds two different approximations for the solution at each step and then compares them. If the two solutions agree closely, the approximation is accepted. If the two answers are not in close agreement according to a specified accuracy, the step size is reduced. However, if the answers agree to more significant digits than required, we increase the step size.

For a dependent variable Φ with y as an independent variable, Runge-Kutta implementation takes the following form:

$$\Phi_{i+1}^{[4]} = \Phi_i + \left(\frac{25}{216}k_1 + \frac{1408}{2565}k_3 + \frac{2197}{4104}k_4 - \frac{1}{5}k_5\right),$$

$$\Phi_{i+1}^{[5]} = \Phi_i + \left(\frac{16}{135}k_1 + \frac{6656}{12825}k_3 + \frac{28561}{56430}k_4 - \frac{9}{50}k_5 + \frac{2}{55}k_6\right);$$

$$k_1 = hf(y_i, \Phi_i),$$

$$k_2 = hf\left(y_i + \frac{1}{4}h, \Phi_i + \frac{1}{4}k_1\right),$$

$$k_3 = hf\left(y_i + \frac{3}{4}h, \Phi_i + \frac{3}{32}k_1 + \frac{9}{32}k_2\right), \tag{26}$$

$$k_4 = hf\left(y_i + \frac{12}{13}h, \Phi_i + \frac{1932}{2197}k_1 - \frac{7200}{2197}k_2 + \frac{7296}{2197}k_3\right),$$

$$k_5 = hf\left(y_i + h, \Phi_i + \frac{439}{216}k_1 - 8k_2 + \frac{3680}{513}k_3 - \frac{845}{4104}k_4\right),$$

$$k_6 = hf\left(y_i + \frac{1}{2}h, \Phi_i - \frac{8}{27}k_1 + 2k_2 - \frac{3544}{2565}k_3 + \frac{1859}{4104}k_4 - \frac{11}{40}k_5\right),$$

where $\Phi_i = \Phi_i^{[5]}$.

It is important to note here that altogether, there are only six function evaluations per step, because the 4th- and 5th-order methods share 5 function evaluations (one of them is for finding k_2, which does not explicitly enter the expressions for $\Phi_i^{[4]}$ and $\Phi_i^{[5]}$, but is used in the evaluation of k_3).

4.1 Analysis of results

The physical parameters entering the problem are $S, M, Gr, Gc, \Pr, Sc, N, R, Ec, L, D_T^t, D_C^c$, which represents each respectively, suction parameter when $S > 0$ or injection when $S < 0$, magnetic parameter, thermal Grashof number, mass Grashof number, Prandtl number, Schmidt number, thermal radiation, reaction parameter, hydrodynamic slip factor parameter, thermal slip factor parameter, and mass slip factor parameter. However, among these parameters only few are presented and discussed in figures and table forms.

In this research, where otherwise stated, the value of the Prandtl number, $\mathbf{Pr} = 0.71$, which represents air at 20 °C is chosen for the investigations. We chose air because it conducts electricity weakly. For the Schmidt number, *Sc*, the value of 0.64 is used which represents an average value of the presence of species by hydrogen (0.22), water vapour (0.60), ammonia (0.78) and carbon-dioxide (0.96). The other parameters used are indicated on the Figures and tables presented, with the solid lines depicting the analytical solutions and the asterisks, the numerical solutions implemented in Maple 18. The graphs and tables are as follows;

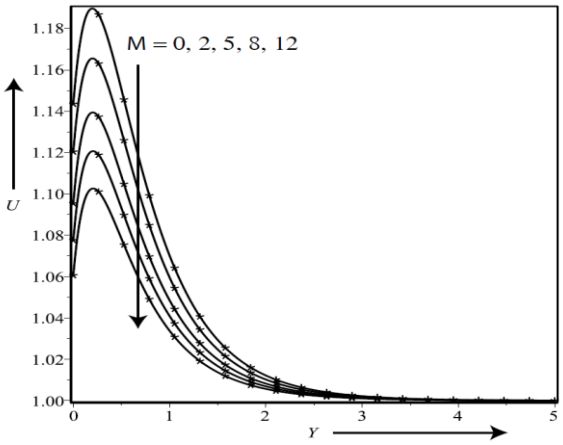

Figure 4.1: Plot of U versus Y with variations of Magnetic parameter for $pr = 0.71, Gr = 2, Gc = 1, Sc = 0.64, N = 2, L = 2, D_T^t = 0.1, D_C^c = 0.1, S = 2, Ec = 0.2, R = 0.2$

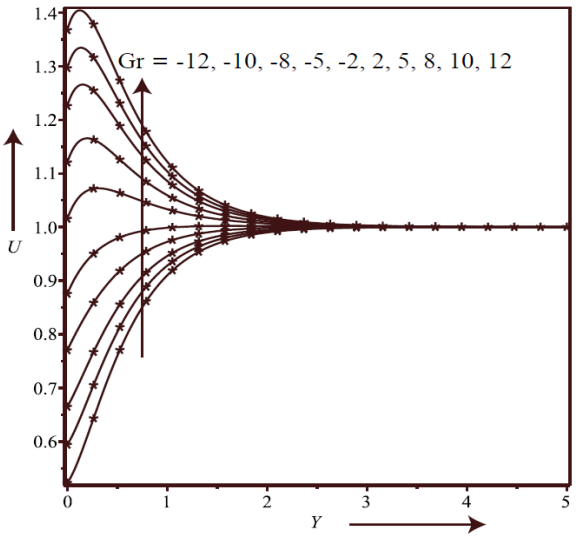

Figure 4.2: Plot of U versus Y with Variations of Grashof number for

$M = 2, \Pr = 0.71, L = 2, Gc = 1, Sc = 0.64, , N = 2, D_T^t = 0.1, D_C^c = 0.1,$
$S = 2, Ec = 0.2, R = 0.2$

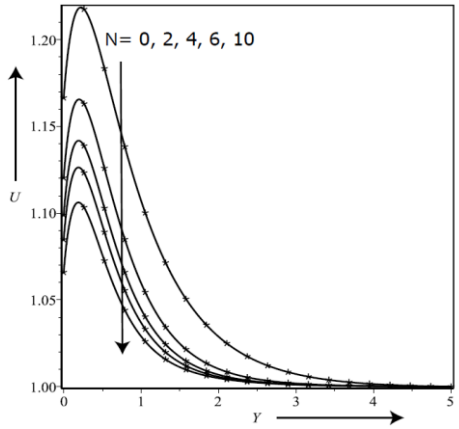

Figure 4.3: Plot of U versus Y with variations of thermal radiation for $M = 2, pr = 0.71, Gr = 2, Gc = 1, Sc = 0.64, N = 2,$ $L = 2, D_T^t = 0.1, D_C^c = 0.1, S = 2, Ec = 0.2, R = 0.2$

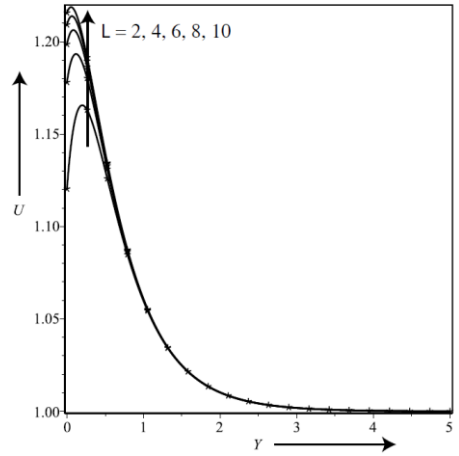

Figure 4.4: Plot of U *versus* Y *with variations of velocity slip factor for* $M = 2, \Pr = 0.71, Gr = 2, Gc = 1, Sc = 0.64, , N = 2, D_T^t = 0.1, D_C^c = 0.1,$ $S = 2, Ec = 0.2, R = 0.2$

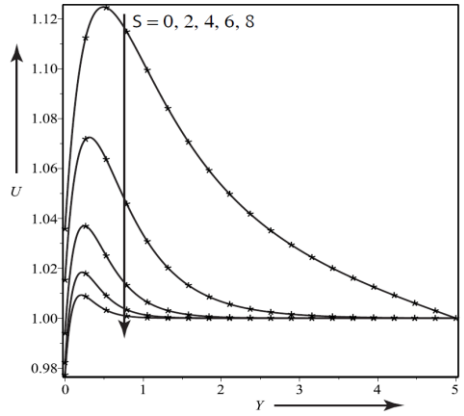

Figure 4.5: Plot of U *versus* Y *with variations of Suction Parameter for* $M = 2, L = 2, pr = 0.71, Gr = 2, Gc = 1, Sc = 0.64,$ $N = 2, D_T^t = 0.1, D_C^c = 0.1, Ec = 0.2$

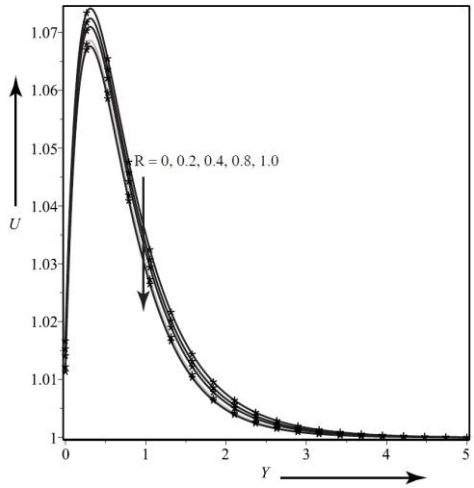

Figure 4.6: Plot of U versus Y with variations of Reaction Parameter for
$M = 2, Gr = 2, \Pr = 0.71, Gc = 1, Sc = 0.64,$
$N = 2, L=2, D_T^t = 0.1, D_C^c = 0.1, Ec = 0.2, S = 2$

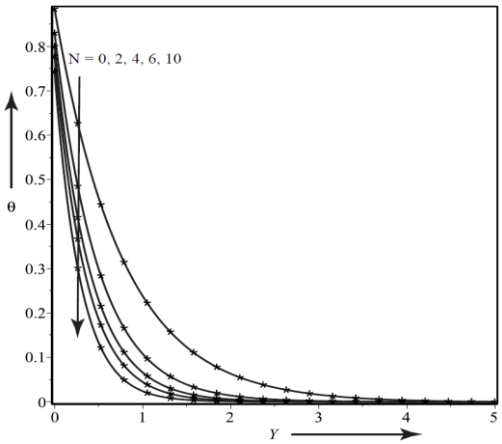

Figure 4.7: Plot of θ versus Y with variations of thermal radiation for:
$M = 2, \Pr = 0.71, Gr = 2, Gc = 1, Sc = 0.64, L = 2, D_T^t = 0.1, D_C^c = 0.1, S = 2, Ec = 0.2, R = 0.2$

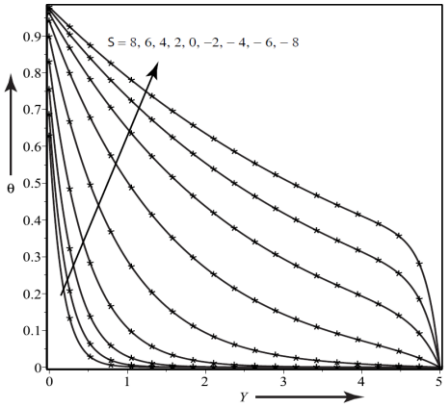

Figure 4.8: Plot of θ versus Y with variations of Suction and Injection Parameter for
$M = 2, L = 2, \Pr = 0.71, Gr = 2, Gc = 1, Sc = 0.64,$
$N = 2, D_T^t = 0.1, D_C^c = 0.1, Ec = 0.2, R = 0.2$

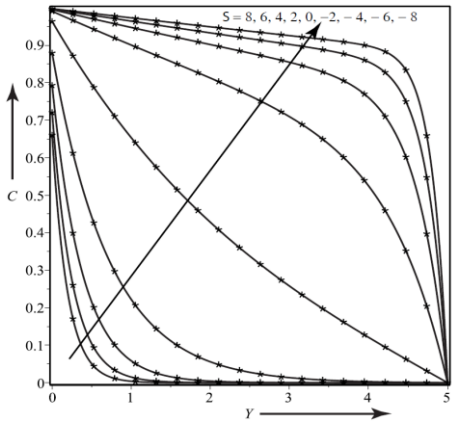

Figure 4.9: Plot of C versus Y with variations of Suction and Injection Parameter for
$M = 2, L = 2, \Pr = 0.71, Gr = 2, Gc = 1, Sc = 0.64,$
$N = 2, D_T^t = 0.1, D_C^c = 0.1, Ec = 0.2, R = 0.2$

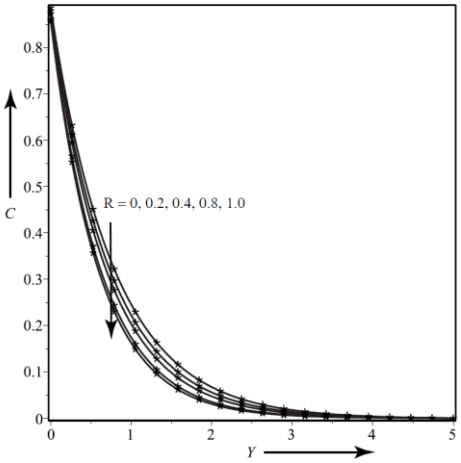

Figure 4.10: Plot of C versus Y with variations of Reaction Parameter for
$M = 2, Gr = 2, \Pr = 0.71, Gc = 1, Sc = 0.64, N = 2,$
$L = 2 D_T^t = 0.1, D_C^c = 0.1, Ec = 0.2, S = 2$

Table 4.1: Effects of Variations of Magnetic parameter on Skin Friction and Heat Transfer for
$\Pr = 0.71, Gr = 2, Gc = 1, Sc = 0.64, N = 2,$
$L = 2, D_T^t = 0.1, D_C^c = 0.1, S = 2, Ec = 0.2, R = 0.2$

M	τ_s, **Skin Friction**	q_θ, **Heat Transfer**
0	0.571768401815826	1.69414788287964
2	0.560185053433064	1.69461626723257
5	0.547683577731952	1.69508048163417
8	0.538782816030583	1.69538563894551
12	0.530269734334842	1.69565932016729

Table 4.2: Effects of Variations of thermal radiation on Skin Friction and Heat Transfer for
$M = 2, \Pr = 0.71, Gr = 2, Gc = 1, Sc = 0.64, L = 2$

N	τ_s, **Skin Friction**	q_θ, **Heat Transfer**
0	0.583258465196805	1.15622387939592
2	0.560185053433064	1.69461626723257
4	0.549470891951255	1.99725574998599
6	0.542382800146564	2.22190755316347
10	0.532937584984608	2.55889055454638

Table 4.3: Effects of Variations of Grashof number on Skin Friction and Heat Transfer for $M = 2, \Pr = 0.71, Gc = 1, Sc = 0.64, N = 2, L = 2,$ $D_T^t = 0.1, D_C^c = 0.1, S = 2, Ec = 0.2, R = 0.2$

Gr	τ_s, **Skin Friction**	q_θ, **Heat Transfer**
-12	0.261335123824823	1.68217075796345
-10	0.296900785484813	1.68592103279430
-8	0.332281715463325	1.68905802988467
-5	0.385084666439434	1.69261896160947
-2	0.437670751984369	1.69481150984757
2	0.507650503203554	1.69561085232571
5	0.560185053433064	1.69461626723257
8	0.612892141856225	1.69225055708556
10	0.648184407140987	1.68990798524958
12	0.683641474033948	1.68694957222031

Table 4.4: Effects of Variations of velocity slip factor on Skin Friction and Heat Transfer for $M = 2, \Pr = 0.71, Gr = 2, Gc = 1, Sc = 0.64, N = 2,$ $D_T^t = 0.1, D_C^c = 0.1, S = 2, Ec = 0.2, R = 0.2$

L	τ_s, **Skin Friction**	q_θ, **Heat Transfer**
2	0.560185053433064	1.69461626723257
4	0.294515963547004	1.69544764955430
6	0.199776206785813	1.69533466477654
8	0.151153768561930	1.69519305874903
10	0.121566518189676	1.69507912697265

Table 4.5: Effects of Variations of Injection and Suction on Skin Friction, Heat and Mass Transfers for $M = 2, Gr = 2, \Pr = 0.71, Gc = 1, Sc = 0.64, N = 2, L = 2,$ $Hs = 2, Ec = 0.2, R = 0.2$

S	τ_s, **Skin Friction**	q_θ, **Heat Transfer**	q_C, **Mass Transfer**
-8	0.447830700592721	0.208937176382697	0.0248173640685261
-6	0.470811149534931	0.269923648189778	0.0329400481193549
-4	0.493124318991862	0.375837054429310	0.0488247558214493
-2	0.511423767671319	0.584129323848656	0.0932934872849105
0	0.517884161455516	1.012480364246150	0.3645453624487080
2	0.507650503203554	1.695610852325710	1.2081512790611900
4	0.496986950070130	2.442882003441330	2.0691974017621200
6	0.491139598720999	3.122070134131310	2.7917791799984400
8	0.488645602306346	3.708608926015520	3.3971080726043100

Table 4.6: Effects of Variations of Reaction Parameter on Skin Friction, Heat and Mass Transfers for M = 2, Gr = 2, Pr = 0.71, Gc = 1, Sc = 0.64, N = 2, Da = 0.1, L = 2, D_T^t = 0.1, D_C^c = 0.1, Hs = 2, Ec = 0.2, S = 2

R	τ_s, **Skin Friction**	q_θ, **Heat Transfer**	q_C, **Mass Transfer**
0.0	0.508340611251478	1.69559491869039	1.13642574153923
0.2	0.507650503203554	1.69561085232571	1.20815127906119
0.4	0.507062276619597	1.69562463224485	1.27118624745958
0.8	0.506091402062647	1.69564773290946	1.37940699057977
1.0	0.505679312100689	1.69565764979695	1.42703272153241

5.1. Discussion of results

We have solved and obtained results for various parameter values of the problem under consideration hence the interpretations. Figure 4.1 depicts the effects of the magnetic parameter on the velocity. It is observed that the velocity reaches a maximum and asymptotically reduces to one at the edge of the boundary layer. Evidently, increase in the magnetic parameter reduces the maximum velocity, thereby causing the boundary layer to be reduced. Physically, the transverse magnetic field plays a similar role to the resistive force (also called Lorentz force) like drag force (which acts in a direction opposite the direction of low of the fluid) thereby opposing the flow and consequently decreases the maximum velocity. It is equally observed that the velocity profiles exhibit jumps at the plate due to the reduced maximum velocity as the magnetic field increases. Consequently, increasing magnetic parameter reduces the skin friction of the fluid, and this is confirmed in the second column of Table 4.1. In Figure 4.2 the effects of the Grashof number is depicted. It is seen that in the range $-12 \leq Gr \leq 12$, on increasing the Grashof number, the maximum velocity occurring close to the plate's edge increases. From the physical point of view, the Grashof number $Gr > 0$ represents the manner in which the plate cools externally due to free convection currents, $Gr < 0$ shows the heating of the plate externally, while, $Gr = 0$ represents the absence of free convection currents.It is observed in Figure 4.3 that the maximum velocity decreases as the thermal radiation increases and this reduces the boundary layer. The physical implication of this is that thermal radiation causes heat transfer to the plate. In other words, thermal radiation brings about heating of the plate by reducing the skin friction at the wall of the plate, and this is confirmed as displayed in the second column of Table 4.2.

Figure 4.4 is a result of variations of hydrodynamic slip factor. Evidently, the observations are that the hydrodynamic slip factor increases the maximum velocity, and this occurs about between 0 and 0.5, and the profiles coalesces and fades away to zero at 5 on the boundary layer. Physically, the hydrodynamic slip factor reduces the skin friction. The effect of suction on the velocity profiles is shown in Figure 4.5. It is observed that as suction increases the maximum velocity reduces, and asymptotes to the velocity far away from the wall of the plate. Also, Figure 4.6 pertains to velocity profiles due to variations in the reaction parameter. Once again, the same features of the velocity profiles are observed, but with minimal effects. Figures 4.7 & 4.8 relate to the temperature profiles with variations of some physical parameters. It is observed in Figure 4.7 that the profiles are all exponentially decreasing such that the magnitude of the maximum temperature occurs at the wall of the plate and decays to zero asymptotically, signifying the characteristics of the boundary conditions. Physically, thermal radiation aids the heating of the plate, thereby increasing the heat transfer. The temperature profiles in view of variations of suction and injection, respectively, are shown in Figure 4.8. It is observed that suction drives the heat to the plate, consequently increasing the heat transfer, whereas injection inhibits the heat transfer by bulging the profiles away from the wall of the plate. Figures 4.9 and 4.10 are concentration profiles due to variations of suction, injection and reaction parameters, respectively. Whereas suction transports the specie to the plate, thereby reducing the mass transfer, injections do the opposite by moving species away from the plate, thereby increasing the mass transfer rate (see Table 4.3).

Figure 4.10 shows the effects of variations of reaction parameter on the concentration profiles. Clearly, an increase in the reaction parameter increases the maximum concentration at the wall of the plate. Physically, increasing reacting specie increases the mass transfer to the wall of the plate, and this is clearly confirmed in the third column of Table 4.8. Tables 4.1 – 4.6 contain the effects of the parameters of Magnetic field, thermal radiation, Grashof number, hydrodynamic slip, suction and injection and reaction on the skin friction, heat and mass transfer coefficients, as indicated respectively. It can readily be deduced from the Table 4.1 that as the magnetic parameter increases, the skin friction reduces, whereas increasing magnetic parameter increases the heat transfer rate. For the thermal radiation, it is observed in Table 4.2 that it reduces the skin friction, whereas the heat transfer rate, the Nusselt number is increased. It is observed in Table 4.3 that for $Gr < 0$, the skin friction reduces together with the rate of heat transfer due to the external cooling of the plate, while for $Gr > 0$ the skin friction increases, and the rate of heat transfer decreases and increases due to the external heating of the plate. Table 4.4 show that the hydrodynamic slip factor reduces the skin friction, but as for the rate of heat transfer, the hydrodynamic slip factor both reduces and increases it. The effects of suction and injection on the rate of heat transfer, rate of mass transfer and the skin friction is considered in Table 4.5. Clearly, the table

shows that both suction and injection reduces the skin friction. However, suction increases both the rates of heat and mass transfers, while, injection decreases both the transfer rates of heat and mass with the effects much more pronounced in the rate of mass transfer. Table 4.6 gives the effects of the chemical reaction parameter on skin friction, heat and mass transfer rates. Obviously as the table depicts, the reaction parameter reduces the skin friction, whereas both heat and mass transfer rates are increased.

6. Conclusion

Analytical Solutions were advanced via Regular Perturbation Method, which were validated by Finite Difference Runge-Kutta Fehlberg numerical experiments using symbolic algebra Package (**MAPLE 18**). It was observed that the governing equations presented considerable mathematical interests for the intended investigations hence the following conclusions were drawn:

(i) That the results represent the characteristics of the problem, whereby the boundary conditions were satisfied both for the velocity, temperature and concentration.

(ii) That the velocity generally steadily increases to a maximum and asymptotically reduces to the ambient far away from the plate

(iii) That the maximum for both the temperature and concentration occur at the wall of the plate, but exponentially decreases to the far boundary.

(iv) That increase in the magnetic parameter reduces the maximum velocity, thereby causing the hydrodynamic boundary layer to be reduced, while magnetic parameter makes no marked difference in the temperature.

(v) That the magnetic parameter reduces the skin friction, while it increases the heat transfer rate.

(vi) That the thermal radiation increases the maximum velocity, whereas it reduces the maximum temperature.

(vii) That thermal radiation parameter decreases the skin friction, while it increases the heat transfer rate.

(viii) That Grashof number plays the role of heating the plate when $Gr < 0$ (i.e. reducing the hydrodynamic boundary layer), whereas $Gr > 0$ implies cooling of the plate, thereby increasing the maximum velocity.

(ix) That suction increases the maximum velocity, while it reduces the maximum temperature and concentration.

(x) That the perturbation analytical and numerical solutions demonstrated excellent agreements.

Reference

[1]. Blasius, H. (1908). The Boundary Layers in fluids with little friction, Z. Math. Phys. 56: 1-37. (English translation).

[2]. Wadsworth, D.C. (1993). Slip effects in a confined rarefied gas II: Velocity and temperature slip, submitted to Phys. Fluids A, 32, 49-59.

[3]. Aral, B.K.; and Kaylon, D.M. (1994). Effects of temperature and surface roughness on time-dependent development of wall slip in steady torsional flow of concentrated suspencions, J. Rheol 38, 957 – 972.

[4]. Sahraoui, M.; and Kaviany, M. (1994). Slip and no-slip temperature boundary conditions at the interface of porous, pane media. International journal of heat and mass transfer, 35(4), 927-943.

[5]. Abbey, T.M. and Bestman, A.R. (1995). Slip flow in a two-component plasma model with radiative heat transfer. Int. J. Energy Research, 19:1-16.

[6]. Rao I. J and Rajagopal K. R (1999). The effect of slip boundary condition on the flow of fluids in a channel, Acta Mech., 135, 113-126

[7]. Mebine, P., (2007). Thermonsolutal MHD flow with radiative heat transfer past an oscillating plate, advances in Theoretical and Applied Mathematics, Vol. 2, No. 3, pp. 217 – 231.

[8]. Martin M. J and Boyd I. J (2008). Momentum and heat transfer in laminar boundary layer with slip flow". Journal of thermophysics and heat transfer 20 (2006) 710 – 719.

[9]. Hayat, T.; Ebraham, M., Fazal, M.M., (2008). Peristaltic MHD flow of third grade fluid with an endo-scope and variable viscocity, Journal of nonlinear mathematical physics 15; sup 1, 91-104.

[10]. Yazdi M H., Abdullah S., Hashim I, Zaharim A., and Sopiam K., (2008). Friction and heat transfer in slip flow boundary layer at constant heat flux boundary conditions. In proceedings of the 10th International conference on Mathematical Methods. Computational Techniques and Intelligent Systems, Corfu, Greece, 26-28 pp 207-212.
[11]. Mebine, P. (2009). Double diffusive convection MHD flow past a vertical porous plate. Journal of Nigerian Association of Mathematical Physics 14(1), 315 – 334.
[12]. Abbas, Z.; Wank, Y.; Hayat, T.; Oberlack, M. (2009). Slip effects and heat transfer analysis in a viscous fluid over an oscillatory stretching surface. Int. J. Numer. Meth. Fluids, Vol. 59, pp. 443-458.
[13]. Fang, T.; Zhang, J.; Yao, S. (2009) Slip MHD viscous flow over a stretching sheet. An exact solution, Comm. Nonlinear Num. Simu., 14, 3731 – 3737.
[14]. Ahuja, A.; Singh, A. (2009). Slip velocity of concentrated suspensions in coquette flow, J. Rheol, Vol. 53, pp. 1461 – 1485.
[15]. Cao, K.; Baker, J (2009). Slip effects on mixed convective flow and heat transfer from a vertical plate, Int. J. Heat Mass Transfer, 52, pp. 3829-3841.
[16]. Hayat, T.; Hina, S.; and Ali, N. (2010b). Simultaneous effects of slip and heat transfer on the peristaltic flow. Communications in Non-linear science and Numerical Simulation 15: 1526-1537.
[17]. Pal D. and Talukdar, B. (2010). Perturbation Analysis of Unsteady Magnetohydrodynamic convective Heat and Mass Transfer in a Boundary Layer slip Flow past a vertical Permeable plate with Thermal Radiation Chemical Reaction, "Communications in Non-linear science and Numerical Simulation, Vol. 15, No. 7, P.P. 1813 – 1830.
[18]. Bhattacharyya, K.; Mukhopadhyay, S.; layek, G.C. (2011). MHD boundary Layer slip flow and heat transfer over a flat plate, Chin. Phys. Lett. 28 (2) 024701.
[19]. Yazdi M H, Abdullah S, Hashim and Sopiam K. (2011). Slip MHD liquid flow and heat transfer over nonlinear permeable stretching surface with chemical reaction. International Journal of Heat and Mass transfer, 5, 3214-3225
[20]. Mebine, P. (2015). Successive Differential coefficients for MHD velocity slip Boundary Layer flow over a plane plaque. Journal of Advances in Mathematics, 10(1) 3098-3107.